ELSEVIER

Materials Characterization 54 (2005) 387–393

MATERIALS CHARACTERIZATION

The use of X-ray diffraction, microscopy, and magnetic measurements for analysing microstructural features of a duplex stainless steel

M.A. Ribeiro Miranda[a,*], J.M. Sasaki[a], S.S.M. Tavares[b], H.F.G. de Abreu[c], J.M. Neto[d]

[a]*Instituto de Física, Universidade Federal do Ceará, Campus do Pici, Caixa Postal 6030, CEP 60455-760 Fortaleza/CE, Brazil*
[b]*PGMEC/TEM, Universidade Federal Fluminense, Rua Passo da Pátria, 156, CEP 24210-240, Niterói/RJ, Brazil*
[c]*Depto. Engenharia Mecânica, Universidade Federal do Ceará, Brazil*
[d]*Instituto de Física, Universidade Federal do Rio de Janeiro, Brazil*

Received 21 October 2004; accepted 28 December 2004

Abstract

X-ray diffraction, light optical microscopy, and magnetization saturation measurements were employed to analyse the microstructural features of a UNS S31803 duplex stainless steel modified by high-temperature treatments. The samples were heated to 1300 °C and cooled by different ways to produce five different microstructures. Solution treatments at 1000 °C were also employed to produce another five conditions. Three methods were employed to determine the austenite/ferrite proportions. X-ray diffraction gave higher austenite values than the other methods, due to the influence of texture, but can be successfully used to determine the microstrain level in each phase. Magnetic saturation measurement is a very simple and precise method for quantification of austenite and ferrite volume fractions in samples that were fast-cooled and slow-cooled. Light microscopy can give a fast and precise measurement of the phase proportions and reveals important features related to the morphology of the phases, but in the samples where the austenite content is low, quantification becomes difficult and imprecise.

Keywords: X-ray diffraction; Magnetic measurements; Duplex stainless steel

1. Introduction

Duplex stainless steels (DSS) and superduplex stainless steels (SDSS) are high-strength corrosion-resistant materials with wide applications in chemical, petrochemical, and nuclear industries. A fine duplex microstructure of austenite islands in a ferritic matrix promotes excellent mechanical properties and corrosion resistance. Optimization of properties of wrought DSS is obtained with the proper control of chemical composition and processing conditions, to obtain about 50% of each phase [1].

During the welding of DSS and SDSS, the main problem is to obtain the desired amount of phases, mainly because high cooling rates tend to produce excessive ferrite in the microstructure. In welding processes,

* Corresponding author.
E-mail address: marcus@fisica.ufc.br (M.A. Ribeiro Miranda).

1044-5803/$ - see front matter © 2005 Published by Elsevier Inc.
doi:10.1016/j.matchar.2004.12.009

excessive ferrite in the heat-affected zone (HAZ) and weld metal (WM) causes a loss of toughness and corrosion resistance [2,3]. An austenite content lower than 25% is unacceptable for most applications [3].

In this context, the characterization of microstructures of DSS with the precise measurement of austenite and ferrite phases assumes great importance. Light microscopy can give a fast phase analysis and also gives information about the morphology and the grain size of each phase. X-ray diffraction analysis can be used to measure the lattice parameters and the microstrain in each phase.

The magnetization saturation measurement can be used to determine the volume fractions of each phase because austenite is paramagnetic and ferrite is ferromagnetic. Mangonon and Thomas [4] have used this method to quantify the magnetic martensite induced by deformation in AISI 304 steel.

In a previous work [5] the following relationship was proposed to measure the ferrite content in UNS S31803 duplex stainless steel:

$$c_\alpha = \frac{m_s\ (\text{emu/g})}{133\ (\text{emu/g})} \tag{1}$$

The value of 133 emu/g is the intrinsic magnetization saturation of a thin sheet of DSS UNS S31803 sample with a 100% ferritic microstructure, produced by water cooling from high temperature.

In this paper, light optical microscopy, magnetization measurement, and X-ray diffraction were applied to analyse the microstructural features of UNS S31803 DSS modified by high-temperature treatments.

2. Experimental

Different UNS S31803 DSS (composition shown in Table 1) microstructures were produced by heat treatments at 1300 °C (30 min) followed by five different cooling procedures: 1—water quenching; 2—oil quenching; 3—air cooling; 4—furnace cooling to 1000 °C and air cooling to room temperature (RT); and 5—furnace cooling to RT. After this, one sample of each condition was heat treated at 1000 °C for 1 h and water cooled, producing five new conditions, resulting in 10 microstructures modified by heat treatment.

Table 1
Chemical composition of the UNS S31803 steel studied

Chemical analysis (wt.%)				
Cr	Ni	Mo	C	N
22.3	5.44	2.44	0.02	0.160

Table 2
Samples identification

Identification	Heat treatment
B1	1300 °C, water cooling to room temperature (RT)
B2	1300 °C, water cooling to RT; solution treatment (1000 °C/h, air cooling)
C1	1300 °C oil cooling to RT
C2	1300 °C oil cooling to RT; solution treatment
D1	1300 °C air cooling to RT
D2	1300 °C air cooling to RT; solution treatment
E1	1300 °C furnace cooling to 1000 °C, air cooling to RT
E2	1300 °C furnace cooling to 1000 °C, air cooling to RT; solution treatment
F1	1300 °C furnace cooling to RT
F2	1300 °C furnace cooling to RT; solution treatment
G1	Melted in arc furnace cooled in refrigerated cooper crucible

Another sample was obtained by melting 5 g of the material, under argon atmosphere, in arc furnace. The solidification occurred in a refrigerated cooper crucible. Table 2 show the identification of the 11 conditions produced for analysis.

All the X-ray measurements were carried out using a PHILIPS® powder diffractometer, model X'Pert Pro, in step-scan mode with step size of 0.02° and time per step of 3 s. It was used with CuK_α (1.54056 A) radiation at 40 kV and 40 mA. In order to keep the beam completely on the sample at low incident angles a divergence slit of 1/2° was used.

The volume fraction of the austenite (γ) and ferrite (α) phases were obtained by the direct comparison method, using the following equations [6]:

$$\frac{I_\alpha}{I_\gamma} = \frac{K_\alpha C_\alpha}{K_\gamma C_\gamma} \tag{2}$$

$$K_{\alpha,\gamma} = \frac{1}{v^2}\left[|F|^2 m\left(\frac{1+\cos^2\theta}{\sin^2\theta\cos\theta}\right)\right]\left(\frac{e^{-2M}}{2\mu}\right) \tag{3}$$

$$C_\alpha + C_\gamma = 1 \tag{4}$$

where: v is the unit cell volume of each phase, F is the structure factor, m is the multiplicity, θ is the reflection angle of the peak analysed, e^{-2M} is the Debye–Waller factor, and μ is absorption coefficient of each phase. Nine measurements were obtained for each condition, using the reflections $(220)_\gamma$, $(111)_\gamma$, $(200)_\gamma$, $(110)_\alpha$, $(200)_\alpha$, and $(211)_\alpha$.

The microstrain (ε) and microstress are related to the peak broadening. The absolute value ϵ can be calculated by the equation [6]:

$$\varepsilon = \frac{\Delta a}{a} = \frac{\beta \cot g\theta}{2} \tag{5}$$

where β is the peak width. In fact, the diffraction peak can be fitted by a pseudo-Voight function, which is a convolution of a Gaussian and a Cauchy function. The peak width of the Cauchy function (β_C) is due to the grain size effect while the peak width of the Gaussian function (β_G) is due to the microstrain of the crystal [7]. The β_G must be so used in Eq. (5) to obtain the microstrain value. In this work, determination of the β_G values followed the procedure suggested by Keijser [7].

The magnetic measurements were carried out in a vibrating sample magnetometer EGG PAR model 4500. Small samples were tested at room temperature, with a maximum applied field of 10 kOe.

Metallographic samples were prepared and etched with hot (90 °C) Murakami's reagent (10 g of potassium ferricyanide, 10 g of potassium hydroxide, and 100 ml of distilled water). The phase quantification was performed using grids of 25 and 16 points, according to the ASTM E 562-89 standard [8].

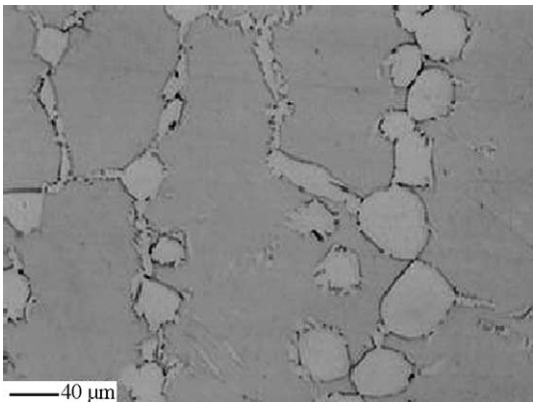

Fig. 1. Microstructure of sample B1.

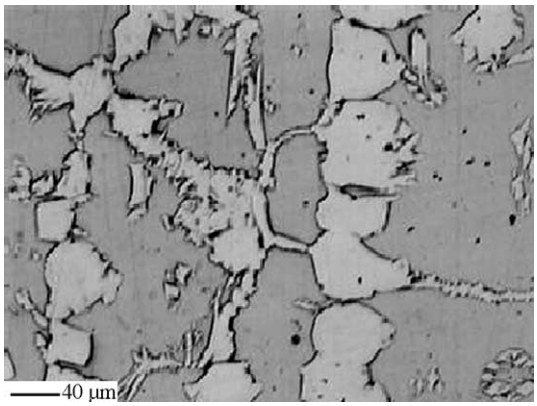

Fig. 2. Microstructure of sample C1.

3. Results

Figs. 1–4 show the microstructures of samples B1, C1, D1, and E1, that were heat-treated at high temperatures. Samples B1 and C1 present polygonal austenite particles and allotriomorph austenite in the grain boundaries. Sample D1 shows these features, but also some Widmanstätten austenite. The slow cooling applied to sample E1 creates the fine biphasic structure with equal parts of each phase. Sample F1 has a microstructure very similar to sample E1.

Figs. 5 and 6 show the microstructures of samples B2 and C2. The heat treatment at 1000 °C promotes the

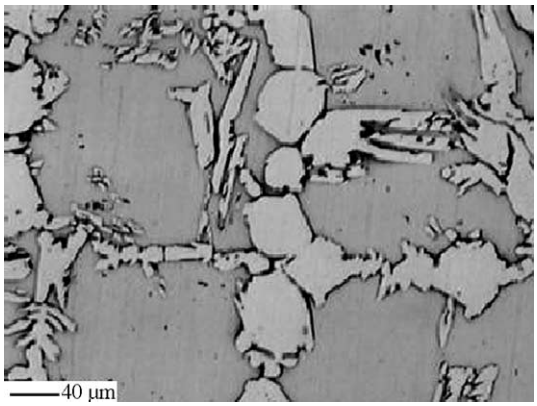

Fig. 3. Microstructure of sample D1.

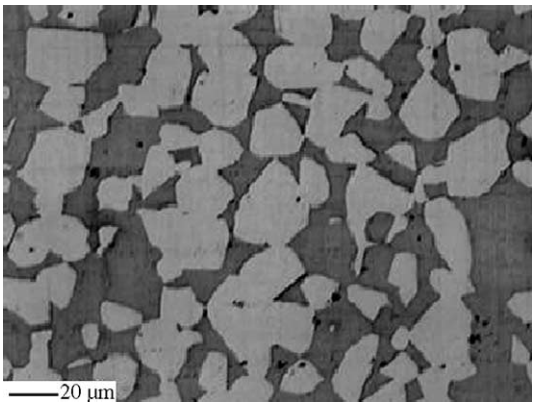

Fig. 4. Microstructure of sample E1.

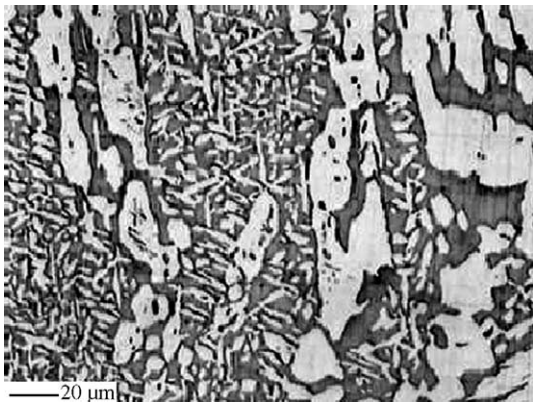

Fig. 6. Microstructure of sample C2.

increase of the austenite volume fraction to the equilibrium values (55–60%). Precipitation occurs inside the ferrite phase, with a desirable grain refinement.

Figs. 7 and 8 show the results of phase quantification using quantitative metallography, X-ray-diffraction and magnetization saturation measurements. The results obtained with microscopy and magnetic measurements agree quite well. The X-ray diffraction quantification gives a higher austenite content, but shows the same variations with the thermal treatment employed.

The microstructure of sample G1, which was remelted in the arc furnace, is shown in Fig. 9. It consists of large ferrite grains with some austenite particles precipitated along the grain boundaries. Of course, this microstructure produced by a very high cooling rate must be avoided in duplex stainless steels due to its poor mechanical properties and corrosion resistance. The precise quantification of this small quantity of austenite by metallography is very difficult. For example, according to the estimate presented in ASTM E-562-99 standard, if the volume fraction is 2% the operator must do 1250 measurements to obtain 10% relative accuracy using a grid of 16 points and 800 measurements for a 25-point grid. The number of measurements falls to 200 if a grid of 100 points is used, but it is still a very large number for practical purposes. X-ray diffraction of sample G1 presents only ferrite peaks, probably because the austenite amount is lower than 5%, which is known to be the average limit of detection by XRD [6]. In this case, quantification by the magnetic method is more suitable. The magnetization saturation of sample G1 was 131.8 emu/g, which correspond to a C_γ=0.009 (0.9%).

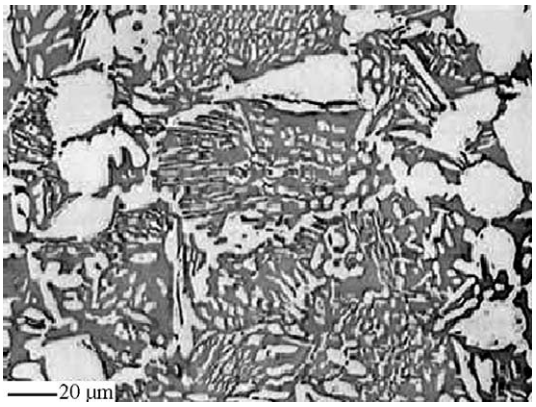

Fig. 5. Microstructure of sample B2.

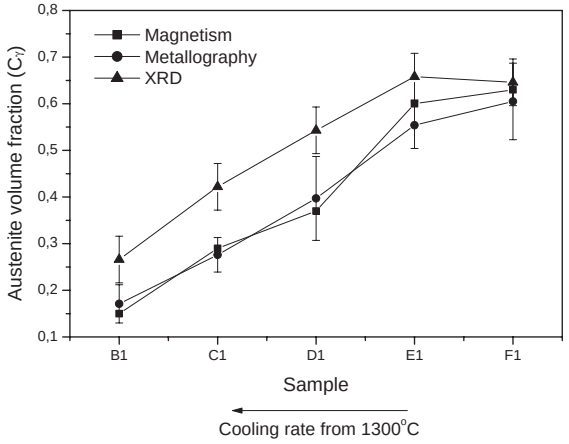

Fig. 7. Austenite volume fractions variation in samples B1 to F1. Comparison between the three methods of quantification.

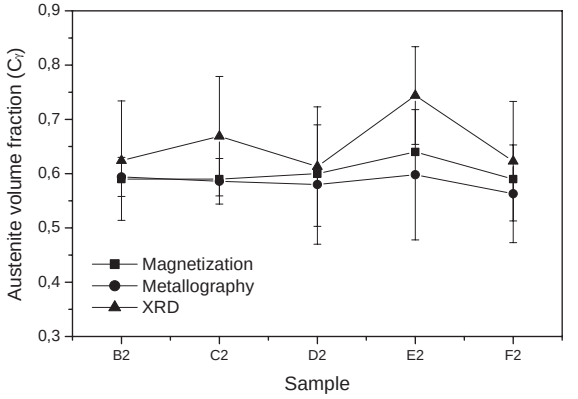

Fig. 8. Austenite volume fractions variation in samples B2 to F2. Comparison between the three methods of quantification.

The magnetic method also gives the most precise result of the three methods. The experimental error in the measurement of the ferrite phase is given by the expression derived from Eq. (1):

$$\Delta C_\alpha = C_\alpha\left(\frac{\Delta m_s}{m_s} + \frac{\Delta m_s}{133}\right) \tag{6}$$

where Δm_s is the experimental error of the m_s measurement estimated as 2% (Δm_s=0.02). Using this expression, the error estimated is less than 1%.

The uncertainty of the light optical microscopical analysis is the statistical error of the n quantifications performed in different regions of the sample. Considering a normal distribution, the error is calculated by [8]:

$$\Delta C_\alpha \text{ or } \Delta C_\gamma = \pm 2\frac{s}{\sqrt{n-1}} \text{ (95\% of confidence)} \tag{7}$$

where s is the standard deviation and n is the number of quantifications. Using this expression, relative accuracies [8] between 5% and 14% were obtained in the measurements by metallography in this work. On the other hand, the metallographic analysis has the advantage of giving important information about other features of the microstructure, such as grain size and morphology. As an example, samples B2 (Fig. 5) and E1 (Fig. 4) present almost the same amount of austenite, but a very different morphology.

The estimated error of the X-ray diffraction measurements were also statistical errors calculated with the nine quantifications performed comparing the selected peaks two by two. The discrepancy of the X-ray diffraction values compared to the other methods employed are attributed to texture of the samples.

The lattice parameters of the two phases were determined by X-ray diffraction. The lattice parameter of the ferrite phase did not change considerably with the heat treatment. Fig. 10 shows the variation of the austenite lattice parameter (a_γ). The increase of the cooling rate from 1300 °C increases the a_γ value, mainly due to the increase of interstitial nitrogen atom concentration in the austenite islands. Collecting XRD data from JCPDS database, it is possible to determine

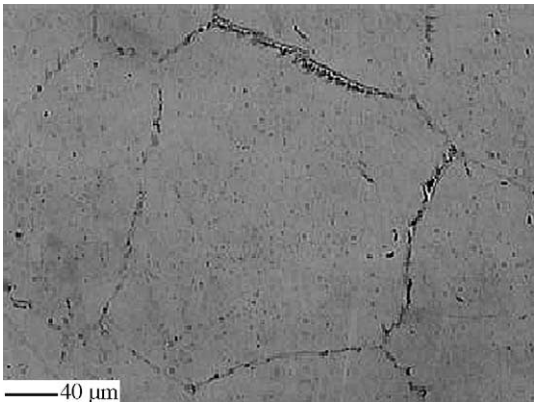

Fig. 9. Microstructure of sample 6A.

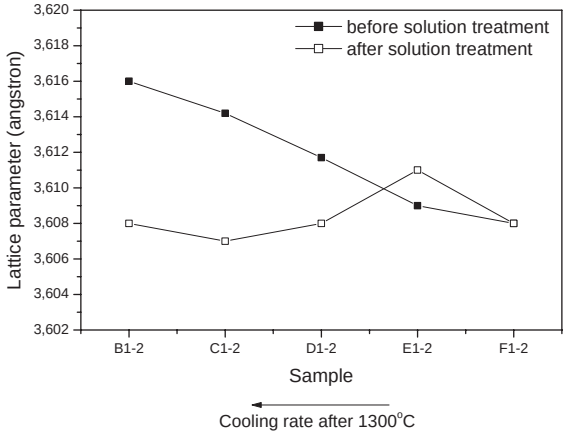

Fig. 10. Austenite lattice parameter variation.

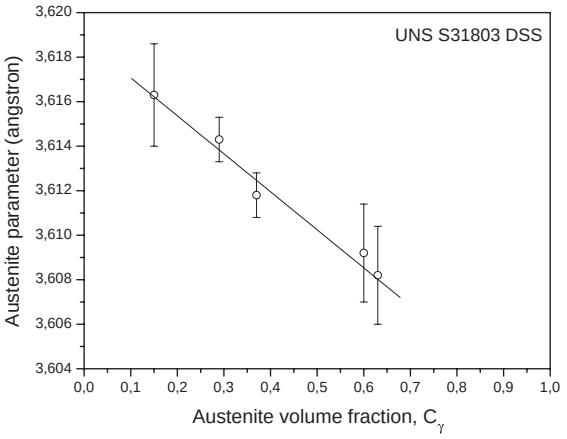

Fig. 11. Austenite lattice parameter versus austenite volume fraction.

the influence of nitrogen on the unit cell volume of Fe-γ (V_γ):

$$V_\gamma = 45.127 + 1.411(\%N) \quad (8)$$

$$\frac{dV_\gamma}{d(\%N)} = 1.411 Å^3 \quad (9)$$

Using Eq. (9), the water-cooled sample (B1) must have about 0.22%N more than the furnace cooled sample.

The lattice parameter of the austenite can be related to the austenite volume fraction by a linear relation, as shown in Fig. 11. This relation can be used as an indirect method for phase quantification in duplex stainless steels. Assuming that magnetization saturation gives the more precise and correct values, its calibration curve may be used to obtain an indirect measure of volume fraction.

Microstrain results are shown in Table 3. The parameter η comes from the fitting by the pseudo-Voight function and varies from 0 to 1: when η=0, the peak is described by a pure Gaussian function, while when η=1, the fitted curve is a Cauchy function and the microstrain is zero [7].

The first observation from the results shown in Table 3 is that the microstrain and microstresses depend on the crystallographic direction in the two phases. Comparing the samples heat treated at high temperature (1300 °C), the microstrain level is much lower in the slowly cooled samples (E1 and F1) than in the fast cooled ones (A1, B1, C1). The solution-treated samples (A2 to F2) all present very low microstrain values. It seems that when the ferrite/austenite proportion and the phases composition is distant from equilibrium, as in A1, B1, and C1, the microstress is considerably high. The solution treatment at 1000 °C promotes austenite precipitation and equilibrium is attained. The fast cooling rate employed after this treatment does not introduce microstrain. The high microstrain and microstress level of the low austenite samples can also contribute to the low corrosion and stress corrosion resistance observed in these microstructures.

4. Conclusions

Duplex stainless steel UNS S31803 modified by high temperatures was analysed by light microscopy,

Table 3
Microstrain measured by X-ray diffraction

Sample	γ [111]		γ [200]		γ [220]		α [110]		α [200]		α [211]	
	η	ε	η	ε	η	ε	η	ε	η	ε	η	ε
B1	0.841	0.09	0.716	0.18	0.841	0.06	0.841	0.07	0.668	0.11	0.970	0
C1	0.450	0.09	0.476	0.14	0.585	0.08	0.450	0.08	0.526	0.10	0.482	0.08
D1	0.690	0	0.199	0.15	0.442	0.06	0.690	0.02	0.495	0.08	0.649	0.03
E1	1.000	0	1.000	0	0.914	0	1.000	0	0.865	0.06	1.000	0
F1	1.000	0	0.839	0.10	1.000	0	1.000	0	1.000	0	0.835	0
B2	1.000	0	1.000	0	0.776	0.06	1.000	0	1.000	0	0.901	0.02
C2	1.000	0	1.000	0	1.000	0	1.000	0	1.000	0	1.000	0
D2	1.000	0	0.779	0.15	0.914	0.08	1.000	0	0.757	0.10	0.923	0
E2	1.000	0	0.909	0.07	0.921	0	1.000	0	1.000	0	0.982	0
F2	1.000	0	1.000	0	1.000	0	1.000	0	1.000	0	1.000	0

X-ray diffraction, and magnetization saturation measurements. The magnetic method gives more accurate results for ferrite and austenite volume fractions for a wide range of microstructures. The X-ray diffraction method provides the measurement of austenite and ferrite lattice parameters and the microstrain level in each phase. The austenite parameter (a_γ) increases with the cooling rate from 1300 °C, since the few austenite islands concentrate high nitrogen levels under these conditions. The austenite parameter decreases linearly with the austenite volume fraction. It is also found that the samples fast cooled from 1300 °C present a high microstrain level. The results of phase quantification by light optical microscopy agreed with the magnetic measurements, but they exhibit higher uncertainty.

References

[1] ASM Speciality Handbook "Stainless Steels"; 1994.
[2] Kordatos JD, Fourlaris G, Papadimitriou G. The effect of cooling rate on the mechanical and corrosion properties of SAF 2205 (UNS 31803) duplex stainless steel welds. Scr Mater 2001;44:401–8.
[3] Hsieh RI, Liou HY, Pan YT. Effects of cooling time and alloying elements on the microstructure of the Greeble-simulated heat affected zone of 22%Cr duplex stainless steels. J Mater Sci Perform 2001;10(5):526–36.
[4] Mongonon PL, Thomas G. Structure and properties of thermal-mechanically treated 304 stainless steel. Metall Trans 1970;1: 1587–94.
[5] Tavares SSM, da Silva MR, Neto JM. Magnetic properties changes during embrittlement of duplex stainless steels. J Alloys Compd 2000;313:168–73.
[6] Cullity BD. Elements of X-ray Diffraction. Addison-Wesley Publishing Company; 1956.
[7] Keijser THD, Mittemeijer EJ, Rozendaal HCF. The determination of crystallite-size and lattice-strain parameter in conjunction with the profile-refinement method for the determination of crystal structures. J Appl Crystallogr 1983;16:309–16.
[8] ASTM E562-89—Standard Test Method for Determining Volume Fraction by Systematic Manual Point Count.